Nanoscale

Accepted Manuscript

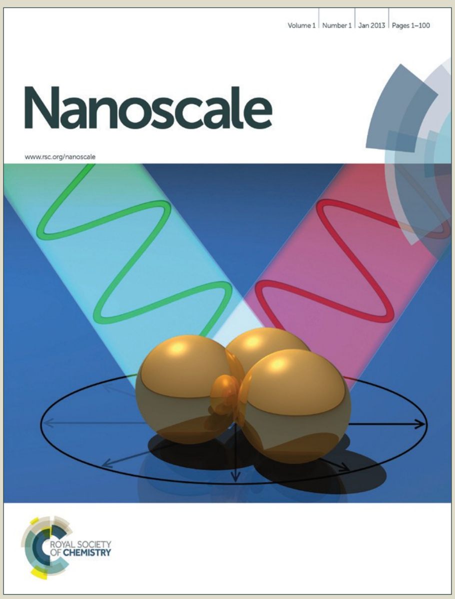

ROYAL SOCIETY OF CHEMISTRY

www.rsc.org/nanoscale

Journal Name

ARTICLE

Novel $MoSe_2$ Hierarchical Microspheres for Applications in Visible-Light-Driven Advanced Oxidation Processes

Received 00th January 20xx,
Accepted 00th January 20xx

DOI: 10.1039/x0xx00000x

www.rsc.org/

Chu Dai[a], Enping Qing[a], Yong Li[a], Zhaoxin Zhou[a], Chao Yang[a], Xike Tian[a]*and Yanxin Wang[b]*

Advanced Oxidation Processes as a green technology has been adopted by combining the semiconductor catalyst $MoSe_2$ with H_2O_2 under the visible radiation . And novel three-dimension self-assembled Molybdenum diselenide ($MoSe_2$) hierarchical microspheres from nanosheets were produced by using an organism, selenium cyanoaceticacid sodium ($NCSeCH_2COONa$), as the source of Se. The obtained products possess a good crystallinity and present hierarchical structures with the average diameter to be 1 µm. The band gap of $MoSe_2$ microspheres is 1.68 eV. And it presents excellent photocatalytic activity under visible light irradiation in the $MoSe_2$-H_2O_2 system. This effective photocatalytic mechanism was investigated in this report which can be attributed to the Visible-Light-Driven advanced oxidation processes.

Introduction

As a green technology, Advanced Oxidation Processes (AOPs) have shown great potential in water environment purification, especially for the application of destroying various organic pollutants, as it can produce large amounts of highly reactive hydroxyl radicals in this process.[1-5] The main problem of AOPs lies in the high cost of reagents such as ozone, or energy light sources like ultraviolet light .[6] What's worse is the separation and recovery of metal ion and formation of precipitate have limited the application of homogeneous Fenton reaction.

H_2O_2 has been widely used in the degradation of organic pollutants as a safe, efficient and easy to use chemical oxidant.[2,7-11] Using of visible–light radiation as an energy source can also reduce costs.Thus,it is important to develop some novel catalyst materials , which could effectively absorb the visible light .And various Fenton-like catalysts based on some metal complexes have been developed recently. This is due to their unique advantages such as facile catalyst recovery from the solution, significant decrease of the material losses.[12,13] Therefore ,Fenton reaction combines the semiconductor-H_2O_2 with the visible radiation produces can be a low-cost, effective way degradation of organic pollutants in water.

Molybdenum diselenide ($MoSe_2$), which belongs to the family of layered transition metal dichalcogenide (LTMD), is an interesting narrow-band-gap semiconductor with a band gap ranging from 1 eV to 2 eV.[14-17] Their layered structure resembles that of graphite with weak van deer Waals interactions between the individual layers. Theoretical band-structure calculation results combine with photoelectron spectroscopy analyses, indicated that the energy gap of $MoSe_2$ (≈1.4eV) matches well with the solar spectrum. And as the optical transitions of $MoSe_2$ are between non-bonding metal d states,it possess high anti-photocorrosion.[15-16] Based on their excellent optical absorption and high anti-photocorrosion properties, $MoSe_2$ has been extensively researched as a novel material which attracted large numbers of researchers in the field of catalyst carrier, electrochemical hydrogen storage and other fields. What's more, 3D hierarchical microstructures, assembled by nanowires or nanosheets, have attracted extensive attention for applications in optoelectronics, solar cells, and photocatalysis. As these microstructures not only have high surface areas, but also can achieve increased stability,better carrier transport capability, and enhanced light scattering.[18]

Recently, $MoSe_2$ nanoparticle have been obtained by various physical and chemical strategies including chemical vapor deposition (CVD),[19-21]electro-deposition,[22] colloidal synthesis,[23] sonochemical synthesis[24] and solvothermal conversions.[25] Most of the methods are very complicated and needs to be carried out under high temperature. Zhou et al[23] synthesized

[a.] Faculty of Materials Science and Chemistry, China University of Geosciences, Wuhan 430074, P. R. China. E-mail: xktian@cug.edu.cn, Tel: +86-27-67884574, Fax: +86-27-67884574.
[b.] School of Environmental Studies, China University of Geosciences, Wuhan 430074, P.R. China. E-mail: yx.wang@cug.edu.cn, Tel: +86-27-87481030, Fax: +86-27-87481030.

Electronic Supplementary Information (ESI) available: [details of any supplementary information available should be included here]. See DOI: 10.1039/x0xx00000x

$MoSe_{2-x}$ nanosheets from the reaction of $MoO_2(acac)_2$ with dibenzyl diselenide which is not easy to obtain such raw materials and costs too much. As we all known , solvothermal conversions is considered to be one of the simplest and most convenient reaction method .Fan et al[25] synthesized $MoSe_2$ flower by adjusting the solution pH to 12 in the hydrothermal reaction process of Na_2MoO_4 and Se in distilled water with hydrazine hydrate. Tang et al[26] obtained $MoSe_2$ nanosheets by hydrothermal reaction of Na_2MoO_4 and hydrazine hydrate -Se in distilled water. However, due to the poor solubility and lower density of selenium often leads to poorly contact between reactants, thus the reaction cannot effectively go on. Besides, hydrazine hydrate presents higher toxicity which is not suitable for extensive use. Therefore, how to prepare hierarchical structures of $MoSe_2$ with rough surface and large surface areas with an economic and safe way still be a challenge.

In this work, 3D self-assembled $MoSe_2$ hierarchical microspheres from nanosheets were produced by using organism $NCSeCH_2COONa$ as the source of Se. The organism Se has charge of minus two, it can easily combined with the reduction of tetravalent molybdenum ions. Besides, compared with inorganic selenium, $NCSeCH_2COONa$ has good solubility in water , which could be a favorable factor for sufficient reaction. And we use ethylene glycol replaced hydrazine hydrate which could reduce the toxicity to a great extent.The obtained products possess a good crystallinity and present hierarchical structures with the average diameter to be 1 μm. What's more, we adopted a green advanced oxidation technology by combining the semiconductor catalyst $MoSe_2$ with H_2O_2 under the visible radiation for destroying organic pollutants. It shows remarkable photocatalytic activity for the degradation of Rhodamine B under visible light irradiation in the $MoSe_2$-H_2O_2 system.

Experimental

Chemicals

All chemicals were of analytical grade and used without further purification.$NCSeCH_2COONa$ was purchased from Wuhan SunEn-Tech Co.,Ltd.

Preparation of $MoSe_2$ microspheres

For the preparation of $MoSe_2$ microspheres: 0.5 mmol $(NH_4)_6Mo_7O_{24}·4H_2O$ (i.e. 3.5 mmol Mo) was dispersed in 30 mL distilled water under constant stirring to form a clear solution. In a separate flask, 7 mmol $NCSeCH_2COONa$ powder was dissolved in 30mL ethylene glycol solvent in open air. When the solution was well mixed, transferred them to an 80 mL Teflon-lined autoclave and heated in an oven at 210�. The black precipitates were collected by centrifugation at 7000 rpm for 5 min, washed with DI water. The washing step was repeated for at least 3 times. Then the products were dry-vacated overnight. Finally, the products were annealed at 450°C in flowing Ar atmosphere for 10 h to yield final crystalline products. After each photocatalysis process, collected the black precipitates by centrifuging at 4000 rpm for 5 min and washed with DI water ,than keep the precipitates dried in a vacuum oven and wait for the next photo-catalytic experiment. Repeated experiments about photocatalytic degradation performance of recycled $MoSe_2$ have done for 3 times.

Characterization

X-ray diffraction (XRD) was used to characterize the crystalline structure of the final product. The chemical compositions of these samples were investigated by X-ray photoelectron spectroscopy (XPS).The surface morphology of the product was studied using field emission scanning electron microscopy (FESEM, Hitachi S-4800), transmission electron microscopy (TEM) and selected area electron diffraction (SAED) using a JEOL 2000 EX apparatus. Ultraviolet-Visible (UV-Vis) spectrophotometer was used to study the optical properties using PerkinElmer Lambda 35 UV/Vis spectrometer.

The photocatalytic activity for the synthesized $MoSe_2$ is evaluated by degradation of Rhodamine B (RhB) solution under visible light irradiation (>420 nm). Before light irradiation, 50 mg photocatalyst $MoSe_2$ was added into 100 mL (20 ppm) RhB solution and the suspensions were magnetically stirred in the dark for 30 min to build up sorption equilibrium. Then 5 mL 30% H_2O_2 was added to promote the catalytic process. Furthermore, all the experiments were performed at room temperature under constant stirring. Every 10 minutes, 10 mL suspension was collected and analyzed with UV–Vis spectrophotometer.

Electron paramagnetic resonance (EPR) analysis

EPR and the spin-trapping technique were used in our study which could be more visually and accurately identification of transient radical intermediates, such as reactive oxygen species (·OH, $O_2·-/HO_2·$, etc).[27] EPR spectra were recorded using a Bruker A300-10/12 EPR spectrometer. In the $MoSe_2$-H_2O_2 system, 0.1 mol spin trapping reagent, 5, 5-dimethyl-1-pyroline-N-oxide (DMPO) was added to 0.5 $mg·mL^{-1}$ $MoSe_2$ suspension solution containing 44 mmol H_2O_2. Then transferred the suspension to an EPR tube immediately before illuminated under visible light (>420 nm) for 3 min. As a control experiment, 0.1 mol DMPO was added to 0.5 $mg·mL^{-1}$ $MoSe_2$ suspension solution, while keep other experimental parameters the same as the $MoSe_2$-H_2O_2 system.

Journal Name

ARTICLE

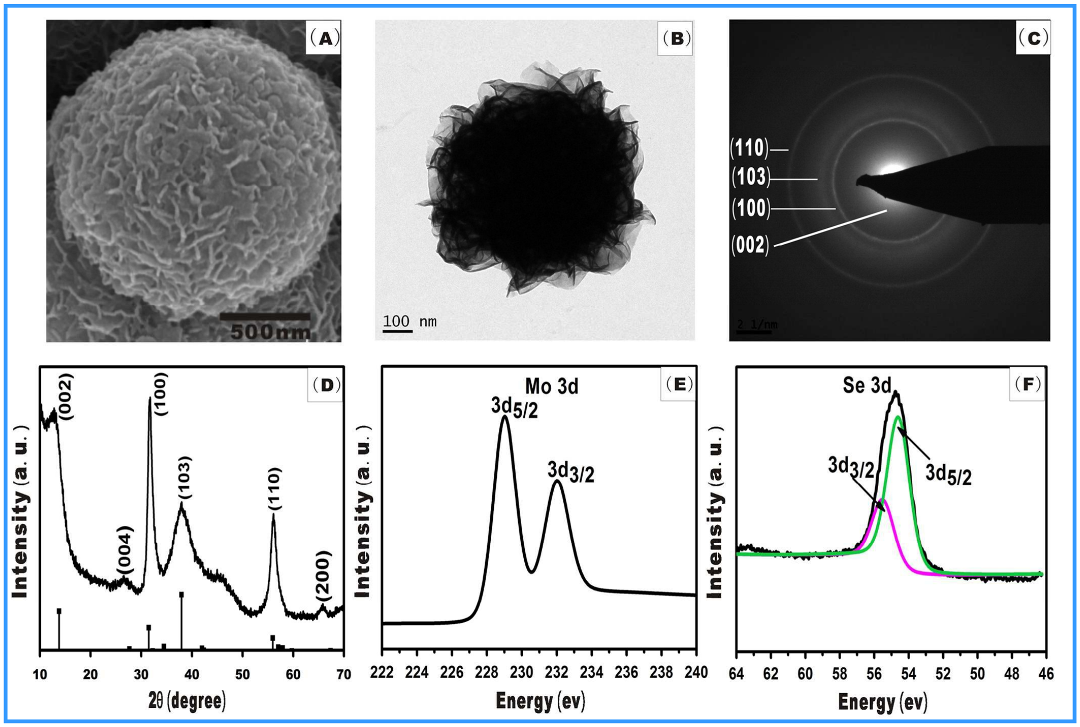

Fig.1 (A) SEM image of $MoSe_2$ microspheres; (B) TEM image of $MoSe_2$ microspheres; (C) SAED pattern of $MoSe_2$ microspheres; (D) XRD patterns of $MoSe_2$ microspheres;(E)High resolution Mo 3d spectra;(F) High resolution Se 3d spectra.

Results and discussion

Structure investigation

Fig.1A shows SEM image of the final $MoSe_2$ microspheres and the average diameter to be 1 μm. Fig.1B shows TEM image of $MoSe_2$ microspheres and it can obviously see the rough surfaces of the hierarchical structures with many sheets on the edge. The accordingly selected area electron diffraction (SAED) pattern was shown in Fig.1C with clear rings indicating the polycrystalline structure to be hexagonal $MoSe_2$. Fig.1D shows the XRD patterns of the as-prepared products. There are more than six intensive diffraction peaks of the synthesized $MoSe_2$ in the two theta range of 10-70° which implies the crystalline nature of this obtained material. And all of the diffraction peaks agree well with the standard pattern of the hexagonal $MoSe_2$ (JCPDS Card, No.77-1775), revealing the high purity of the as-synthesized product. Chemical compositions analysis of these materials was further investigated by X-ray photoelectron spectroscopy (XPS). As shown in Fig.1E, two characteristic peaks arising from Mo 3d5/2 and Mo 3d3/2 orbital are located at 228.8 eV and 232 eV, confirming that molybdenum is in its Mo (IV) state. Whereas the binding energies of Se 3d5/2 and Se 3d3/2 are 54.6 eV and 55.3 eV in Fig.1F, revealing the -2 oxidation chemical state of Se .[28-30]

Growth mechanism of the 3D $MoSe_2$ hierarchical microspheres

The reaction process can be clear seen in Fig.2. First, under the reaction temperature, the ethylene glycol would lose a molecule of water and turn to acetaldehyde.[31,32] Besides, the $NCSeCH_2COONa$ can decompose to H_2Se, CO_2 and NH_3 in this acid solution system. Then the Mo^{6+} can be reduced to Mo^{4+} by acetaldehyde. Finally the Mo^{4+} would combine with Se^{2-} which forms $MoSe_2$.

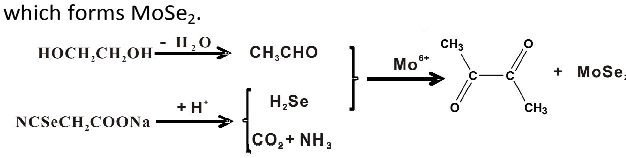

Fig.2 The reaction process of forming the final $MoSe_2$ microspheres.

We can clear see the dynamic change of $MoSe_2$ as shown in Fig.3. Fig.3A-D show a typical SEM image of the as synthesized $MoSe_2$ microspheres under different reaction time for 6 h, 9 h, 12 h and 24 h, respectively. After reaction for 4 hours, there are many nanosheets generated. With time prolonging, the nanosheets tend to aggregate under the influence of the hydrogen bonding interaction and thermodynamic stability. The surface morphology can be seen in Fig.3B, C. Finally, after reacted for 24 hours, it formed the 3D hierarchical microspheres $MoSe_2$ as shown in Fig.3D. Fig. 3E shows the XRD patterns of $MoSe_2$ microspheres under the reaction time for 6 h, 9 h, 12 h and 24 h. And it matches well with the standard pattern of the hexagonal $MoSe_2$ (JCPDS Card, No.77-1775) as mentioned before. Besides , we can clearly see that when the reaction time is short, the crystallization of the product is not good as a intermediate. And the diffraction peak located at 13°was less obviously observed ,indicating a certain degree of amorphous state of this nanosheets $MoSe_2$. With time prolonging , the peaks of the XRD patterns became more sharp and strong ,which implies the crystallization degree of this product gradually improved.And there are no impure peaks of all this XRD patterns of $MoSe_2$,indicating the high purity of the as-synthesized product. Detailed growth mechanism of the 3D $MoSe_2$ microspheres can be described in Fig.3F. In the initial phase reaction, there are many cores will be generated. Because $MoSe_2$ crystal has a nature of layered structure, the core tends to be grown into more nanosheets. Due to the hydrogen bonding interaction and thermodynamic stability, the nanosheets tend to aggregate and finally formed the 3D hierarchical microspheres-like $MoSe_2$.

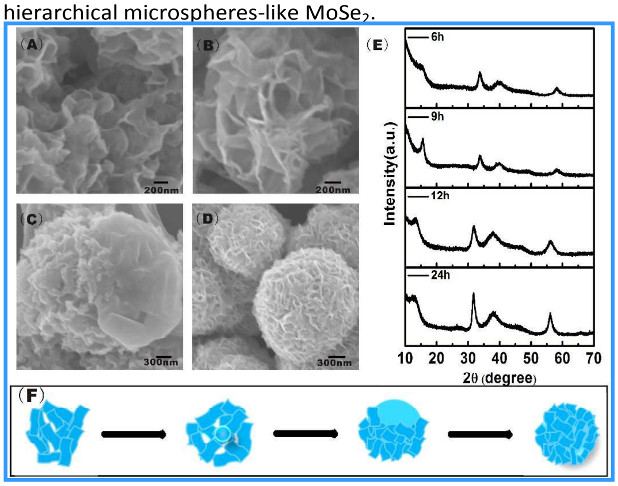

Fig.3 FESEM images of $MoSe_2$ samples obtained at different reaction time: (A) 6 h, (B) 9 h, (C) 12 h, (D) 24 h; (E) XRD patterns of $MoSe_2$ microspheres under the reaction time for 6 h, 9 h, 12 h and 24 h; (F) Schematic illustration of growth mechanism for the formation of $MoSe_2$ microspheres.

Photocatalytic activity

The intrinsic electronic properties including the band edge potential, the band gap, and the charge-carrier mobility of photocatalyst are one of the most important factors in the photocatalytic process.[33] Fig.4 shows the UV-Vis diffuse reflectance spectra of 3D $MoSe_2$ microspheres from 200 nm to 900 nm. And the band gap is calculated to be 1.68 eV.

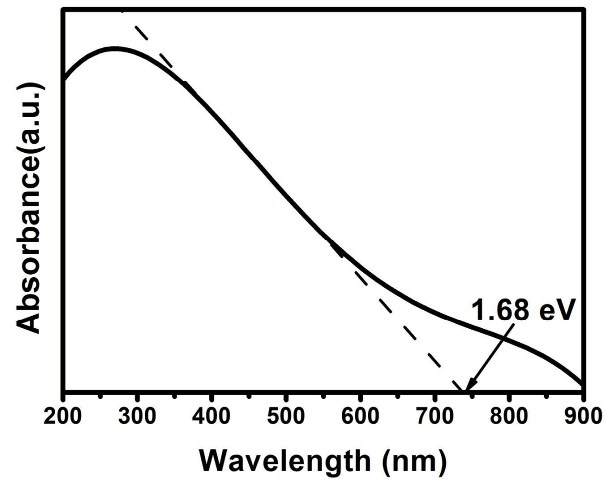

Fig.4 UV-Vis diffuse reflectance spectra of as-synthesized $MoSe_2$ microspheres.

Fig.5A shows the photocatalytic activity for the degradation of RhB under visible-light illumination at different solution system. The RhB solution degrade quickly in the $MoSe_2$-H_2O_2 system (pH=2.51) under visible-light. And it fits a pseudo-first order kinetic model, as described in Eq. (1):

$$\ln\frac{C_0}{C} = Kt \quad \text{Eq. (1)}$$

Where C_0 is the initially concentration of RhB (ppm) and C is the concentration at different light irritation time, K is the pseudo first order reaction rate constant (min^{-1}). Therefore, the rate constant of this photocatalysis process in the $MoSe_2$-H_2O_2 system is about 1.07×10^{-1} min^{-1}.

However, in a separate $MoSe_2$ or H_2O_2 system, it seems no catalytic activity under the same condition. In order to investigate the degradation mechanism, we used 0.01 $mol\cdot L^{-1}$ HCl solution to replace the H_2O_2 solution and adjust the solution pH to the same as that after adding H_2O_2. There seems have litter effect on the degradation of $MoSe_2$. Thus it could not be the acidic property of H_2O_2 solution that affected the photocatalytic activity.

The inset image in Fig.5A shows the evolution of the RhB absorption spectroscopy of the $MoSe_2$-H_2O_2 system exposed to visible light at different irradiation time. The absorption peaks of the RhB solution at 553 nm decreased sharply during the photodegradation process which indicating that the 3D $MoSe_2$ hierarchical microspheres present excellent photocatalytic activity in the presence of H_2O_2.

In order to study the stability of the $MoSe_2$ microspheres in the photocatalysis process. We did repeated experiments about photocatalytic degradation performance of recycled $MoSe_2$ for 3 times. And it can still keep remarkable photocatalytic activity for the degradation of Rhodamine B under visible light irradiation in the $MoSe_2$-H_2O_2 system which can be seen in Fig.5B. And the degradation rate can still up to 90% after 40 min under visible light irradiation in the $MoSe_2$-H_2O_2 system.

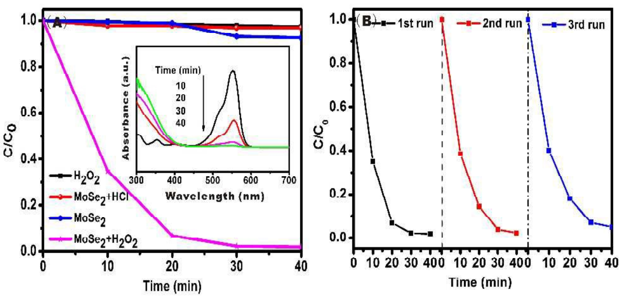

Fig.5 (A)Photocatalytic activities for the degradation of RhB under visible-light illumination in different solution system and the evolution of the RhB absorption spectroscopy of the $MoSe_2$-H_2O_2 system exposed to visible light at different radiation time (inset); (B) The cyclic photocatalytic performance .

The mechanism of H_2O_2 promoted photocatalysis process

As we all known, active radicals, such as hydroxyl radicals (·OH), super oxygen ions (O_2^-) and electron holes (h^+),have played important roles in the photocatalysis process. In order to study the mechanism of this photocatalytic active, we investigated the photodegradation performance of $MoSe_2$ under visible light by control experiments involving the scavenger agents isopropyl (effectively scavenge of ·OH), and triethanolamine (effectively scavenge of h^+).Their photocatalytic activities were shown in Fig.6.

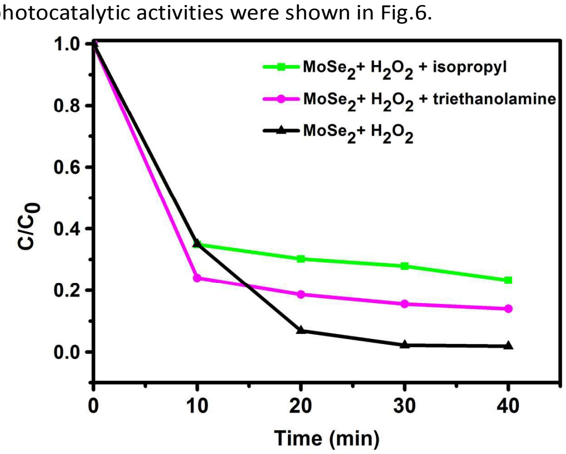

Fig.6 Photocatalytic activities by adding different scavenger agents.

After adding 10 mmol scavenger agents isopropyl and triethanolamine to 100 mL (20 mg·L^{-1}) RhB solution containing 50 mg $MoSe_2$ and 5mL 30% H_2O_2, the degradation rate decreased. As one of the effective scavenge of active radicals, isopropyl would effectively scavenge of ·OH in the photocatalytic process , which could significantly suppressed photodegradation of RhB. And at the same time, as an effective scavenge of h+, when adding triethanolamine to this photocatalytic process, it would also suppressed photodegradation of RhB. The corresponding rate constants for Isopropy-H_2O_2 system,Triethanolamine-H_2O_2 system and H_2O_2 system were $3.1\times10^{-2}min^{-1}$,$4.3\times10^{-2}min^{-1}$,$1.07\times10^{-1}min^{-1}$, respectively,which were shown in Table 1. And we can clear see the rate constants after adding isopropyl is smaller than adding triethanolamine,indicating the isopropyl has greater inhibitory effect in the photocatalytic process, in other words, ·OH is the main active group in this photocatalysis process compare with h^+.

Table 1 Rate constants corresponding to adding different scavenger agents into the H_2O_2-$MoSe_2$ system with $MoSe_2$ concentration to be 0.5 g·L^{-1}.The reaction was carried out under visible light at room temperature and initial concentration of RhB was 20 mg·L^{-1}

Scavenger agents	Duration time(min)	Degradation (%)	Kinetic constant, K (min^{-1})
Blank	40	98.12	1.07×10^{-1}
Triethanolamine	40	86.05	4.3×10^{-2}
Isopropyl	40	76.74	3.1×10^{-2}

To further explore whether the active radical ·OH or the O_2^- is the main active group that promotes this photocatalysis process. EPR and the spin-trapping technique were used in our study which could be more visually and accurately explain the main active group in this photocatalytic process.

EPR spectra obtained after visible-light irradiation of DMPO in $MoSe_2$ system and $MoSe_2$ + H_2O_2 system were shown in Fig.7. And there are four main characteristic peaks and the relative peak magnitudes of 1:2:2:1. The peak locations and the peak magnitudes are consistent with many of the results reported in literatures,which could explain the form of DMPO–OH.[34-40] Therefore, we could draw a conclusion that ·OH rather than the O_2^- was the main active group in this photocatalytic process after adding H_2O_2.

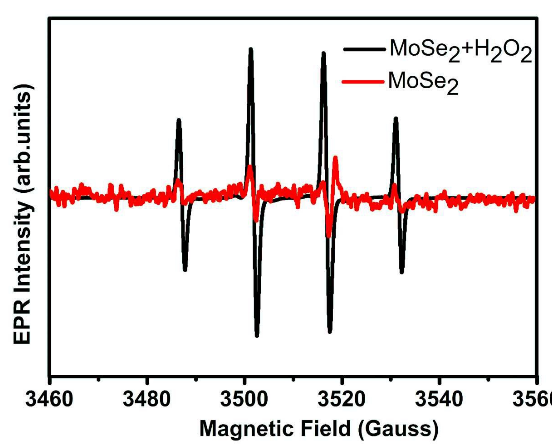

Fig.7 EPR spectra obtained upon visible light irradiation of DMPO in either $MoSe_2$ system or in $MoSe_2$+ H_2O_2 system.

In order to explain how the active radicals of ·OH affect the photocatalytic process. We should understand the whole photocatalysis process first, which is shown in Fig.8A. First, the RhB molecules were absorbed on the surface of 3D $MoSe_2$ microspheres. When added H_2O_2 to $MoSe_2$ suspension, the H_2O_2 molecules can photolysis and generate more active species (·OH). Then these active species would degrade RhB to CO_2 and H_2O.

The detailed mechanism can be described in Fig. 8B. And we will explain the detailed mechanism combine with the source of this active species of ·OH radicals.

When the energy of an incident light exceeds the band gap of $MoSe_2$ (about 1.68 V) during the photocatalysis process, electrons in the valence band will be excited into the conduction band (e_{CB}), leaving holes in the valence band (h_{VB}).

The first source attributed to H_2O_2 can be reduced by e_{CB} on the surface of $MoSe_2$. For the inorganic semiconductor, the positions of conductive band and valence band relative to zero electoral site can be calculate according to the Eq. (2).[41]

$$E_{CB} = X - Ee - 0.5\ Eg \quad \text{Eq. (2)}$$

$$E_{VB} = Eg + E_{CB} \quad \text{Eq. (3)}$$

Where E_{CB} is the conduction band edge potential, X is the electronegativity of the semiconductor, Ee is the energy of free electrons on the hydrogen scale (~4.5 eV), and Eg is the band gap energy of the semiconductor.So the bottom of the conduction band E_{CB} is calculated to be -0.2 V for $MoSe_2$. When the $MoSe_2$-H_2O_2 system is irradiated by visible-light , the photo-excited electrons would across from the valence band to conduction band and react with the dissolved oxygen. Since the reduction potential of O_2·/ HO_2· is about -0.13 V (vs. NHE), the dissolved oxygen would combine with a H^+ that forms HO_2^-, this unstable HO_2^- would finally evolution of ·OH, which is shown in Eq. (4):[42-44]

$$O_2 + e^- + H^+ \rightarrow HO_2\cdot \rightarrow \cdot OH \quad \text{Eq. (4)}$$

$$H_2O_2 + e_{CB} \rightarrow \cdot OH + OH^- \quad \text{Eq. (5)}$$

$$H_2O + h_{VB} \rightarrow H^+ + \cdot OH \quad \text{Eq. (6)}$$

There are also some photo-excited electrons would combine with H_2O_2 molecular and reduce H_2O_2 to ·OH as the reduction potential of H_2O_2/·OH is about 0.87 V (vs. NHE),which is consistent with the literature.[45-47] And this is the second but the main source of ·OH radicals.

When the $MoSe_2$-H_2O_2 system is irradiated by visible-light ,the photo-excited electrons would across from the valence band to conduction band and leaving holes in the valence band (h_{VB}). The holes react with H_2O molecular ,which could be the other path to generate ·OH, the reaction process is shown in Eq. (6). However,the VB edges of $MoSe_2$ is calculated to be 1.48 V according to Eq. (3) which is too low to oxide RhB. Besides,as this low pH value of the reaction solution, the concentration of OH^- was very low and the oxidation of OH^- with h_{vb} to generate ·OH could be neglected.

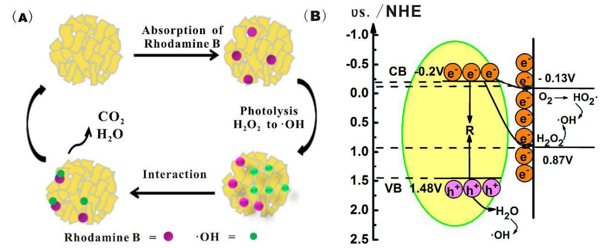

Fig.8 (A)The whole photocatalysis process; (B) Schematic diagram of the detailed degradation mechanism.

Above all,we can briefly explained the mechanism to be the catalysis by the $MoSe_2$ which promote H_2O_2 to generate more ·OH under visible-light irradiation.Besides, it effectively promotes the separation of pairs of electrons and holes by absorption of electrons or holes thus reduce their composite probability.

Conclusions

In summary, novel 3D structure $MoSe_2$ hierarchical microspheres were produced by using an organism, selenium cyanoaceticacid sodium ($NCSeCH_2COONa$) as the source of Se. The transition from nanosheets to the sphere-like structure is attributed to the self-assembly growth. UV-Vis diffuse reflectance spectra indicate that the band gap of $MoSe_2$ to be 1.68 eV. And it shows remarkable photocatalytic activity in the $MoSe_2$-H_2O_2 system under visible light irradiation. The rate constant of this photocatalysis process in the H_2O_2 system is about 1.07×10^{-1} min^{-1}. Combined with a series of control experiments of removing the active groups and EPR technique, we draw a conclusion that this effective photocatalysis process should attribute to Visible-Light-Driven Advanced Oxidation Processes. And the catalysis by $MoSe_2$ microspheres under visible light irritation promotes the photolysis process of H_2O_2 to generate more active group ·OH, thus showing excellent photocatalytic performance. This work implies that $MoSe_2$ has great value in photocatalysis field. And we believe that these $MoSe_2$ might find various potential applications in the areas of catalysis, optics, electronics and sensors.

Acknowledgments

This work was financially supported by the National Basic Research Program of China (973 Program, grant No. 2011CB933700) of the Ministry of Science and Technology of China, the national Nature science Foundation of China (grand No.51371162), the Fundamental Research Funds for the Central Universities.

Notes and references

1.D. F. Ollis, 1993, 518, 18-34.
2.Y. Nie, C. Hu, J. Qu and X. Hu, *J Hazard Mater*, 2008, 154, 146-152.
3.M. Pera-Titus, V. García-Molina, M. A. Baños, J. Giménez and S. Esplugas, *Applied Catalysis B: Environmental*, 2004, 47, 219-256.
4.J. Li, W. Ma, Y. Huang, X. Tao, J. Zhao and Y. Xu, *Applied Catalysis B: Environmental*, 2004, 48, 17-24.
5.N. Quici, M. E. Morgada, G. Piperata, P. Babay, R. T. Gettar and M. I. Litter, *Catalysis Today*, 2005, 101, 253-260.
6.S. Esplugas, J. Gimenez, S. Contreras, E. Pascual and M. Rodríguez, *Water research*, 2002, 36, 1034-1042.
7.N. S. Orang, *American Journal of Physical Chemistry*, 2014, 3, 26.
8.S. Tanioka, Y. Matsui, T. Irie, T. Tanigawa, Y. Tanaka, H. Shibata, Y. Sawa and Y. Kono, *Bioscience, biotechnology, and biochemistry*, 1996, 60, 2001-2004.
9.C. Qin, L. Xiao, D. U. Yumin, M. Fan and X. Shi, *Wuhan University Journal*, 2000,46,195-198.
10.C. Qin, Y. Du and L. Xiao, *Polymer Degradation and Stability*, 2002, 76, 211-218.
11.Y.-h. Lu, G.-s. Wei and J. Peng, Chinese J. Polym. Sci., 2004, 22, 439-444.
12.S. Campestrini and B. Meunier, *Inorganic Chemistry*, 1992, 31, 1999-2006.
13.S. Parra, V. Nadtotechenko, P. Albers and J. Kiwi, *The Journal of Physical Chemistry B*, 2004, 108, 4439-4448.
14.Y. Shi, C. Hua, B. Li, X. Fang, C. Yao, Y. Zhang, Y.-S. Hu, Z. Wang, L. Chen, D. Zhao and G. D. Stucky, *Advanced Functional Materials*, 2013, 23, 1832-1838.
15.R. Coehoorn, C. Haas, J. Dijkstra, C. J. F. Flipse, R. A. de Groot and A. Wold, *Physical Review B Condensed Matter*, 1987, 35, 6195-6202.
16.R. Coehoorn, C. Haas and R. A. De Groot, *Physical Review B Condensed Matter*, 1987, 35, 6203-6206.
17.M. Pumera, Z. Sofer and A. Ambrosi, *Journal of Materials Chemistry A*, 2014, 2, 8981-8987.
18.G. Han, Z.G. Chen, D. Ye, L. Yang, L. Wang, J. Drennan, J. Zou, *J.Mater.Chem.A*, 2 (2014) 7109-7116.
19.J.C. Shaw, H. Zhou, Y. Chen, N.O. Weiss, Y. Liu, Y. Huang, X. Duan, *Nano Research*, 2014, 7, 1-7.
20.X. Wang, Y. Gong, G. Shi, W. L. Chow, K. Keyshar, G. Ye, R. Vajtai, J. Lou, Z. Liu and E. Ringe, *ACS nano*, 2014, 8, 5125-5131.
21.Y. N. Ko, S. H. Choi, S. B. Park and Y. C. Kang, *Nanoscale*, 2014, 6, 10511-10515.
22.L. Jia, X. Sun, Y. Jiang, S. Yu and C. Wang, *Advanced Functional Material*s, 2015, 25, 1814-1820.
23.X. Zhou, J. Jiang, T. Ding, J. Zhang, B. Pan, J. Zuo and Q. Yang, *Nanoscale*, 2014, 6, 11046-11051.
24.M. Fenik and M. Kristl, *Inorganic Chemistry Communications*, 2003, 6, 68–70.
25.C. Fan, Z. Wei, S. Yang and J. Li, *RSC Advances*, 2014, 4, 775-778.
26.H. Tang, K. Dou, C. C. Kaun, Q. Kuang and S. Yang, *Journal of Materials Chemistry A*, 2013, 2, 360-364.
27.Z. Wang, W. Ma, C. Chen, H. Ji and J. Zhao, *Chemical Engineering Journal*, 2011, 170, 353-362.
28.Y. Shi, J.-K. Huang, L. Jin, Y.-T. Hsu, S. F. Yu, L.-J. Li and H. Y. Yang, *Scientific reports*, 2013, 3.
29.T. Ueno, *Japanese Journal of Applied Physics*, 1983, 1469-1473.
30.C. Xu, S. Peng, C. Tan, H. Ang, H. Tan, H. Zhang and Q. Yan, *J. Mater. Chem. A*, 2014, 2, 5597-5601.
31.F. Fievet, J.P. Lagier, B. Blin, B. Beaudoin, M. Figlarz, *Solid State Ionics*, 32-3 (1989) 198-205.
32.L. Ma, Y. Tian, C. Yang, Y. Li, Z. Zhou, Y. Liang, X. Tian, Y. Wang, *Crystengcomm*, 17 (2015) 7056-7062.
33.X. Tu, S. Luo, G. Chen and J. Li, *Chemistry*, 2012, 18, 14359–14366.
34.T. Uchino, H. Tokunaga, M. Ando and H. Utsumi, *Toxicology in Vitro*, 2002, 16, 629–635.
35.V. Krishna, D. Yanes, W. Imaram, A. Angerhofer, B. Koopman and B. Moudgil, *Applied Catalysis B: Environmental*, 2008, 79, 376-381.
36.M. Y. Guo, A. M. C. Ng, F. Liu, A. B. Djurišić and W. K. Chan, *Applied Catalysis B Environmental*, 2011, 107,150–157.
37.T. Wu, T. Lin, J. Zhao, H. Hidaka and N. Serpone, *Environ.sci.technol*, 1999, 33, 1379-1387.
38.M. D. Hernández-Alonso, A. B. HungrA, A. MartNez-Arias, M. Fernández-GarcA, J. M. Coronado, J. C. Conesa and J. Soria, *Applied Catalysis B Environmental*, 2004, 50, 167-175.
39.J. M. Coronado, A. J. Maira, A. MartNez-Arias, J. C. Conesa and J. Soria, *Journal of Photochemistry & Photobiology A Chemistry*, 2002, 150, 213-221.
40.R. F. Zhang, X. K. Tian, L. L. Ma, C. Yang, Z. X. Zhou, Y. Wang and S. Wang, *RSC Advances*, 2015, 45165-45171.
41.H. Cheng, B. Huang, X. Qin, et al. *Chemical Communications*, 2012, 48, 97-99.
42.A. Mills, S.L. Hunte, *Journal of Photochemistry & Photobiology A Chemistry*, 108 (1997) 1–35.
43. Heller A, Acc.chem.res, 28 (1995) 503-508.
44. D. Chatterjee, S. Dasgupta, *Journal of Photochemistry & Photobiology C Photochemistry Reviews*, 6 (2005) 186-205.
45.P. Wardman, *Journal of Physical & Chemical Reference Data*, 1989, 18, 1637-1755.
46.T. Hirakawa and Y. Nosaka, *Langmuir*, 2002, 18, 3247-3254.
47.Y. Du, L. Zhao and Y. Zhang, *J Hazard Mater*, 2014, 267, 55-61.